Chronopotentiometric study of a Nafion membrane in presence of glucose

Y. Freijanes[a], V. M. Barragán*[,a], S. Muñoz[b]

[a]*Department of Applied Physics*

[b]*Department of Applied Physics III*

Faculty of Physics, University Complutense of Madrid, 28040 Madrid, Spain.

*Corresponding author. Fax: +34913945191; e-mail: vmabarra@ucm.es

ABSTRACT

Chronopotentiometric and swelling experiments have been conducted to characterize the behavior of a Nafion membrane in NaCl and KCl aqueous solutions without and with glucose. A mixture solution with similar composition to the cerebrospinal fluid and blood plasma has also been studied. From the chronotentiograms, current-voltage curves have been obtained, and the values of the limiting current density, diffusion boundary layer thickness, difference between counter-ion transport number in membrane and free solution, and transition times have been determined for the investigated membrane systems. The obtained results indicate that the presence of glucose affects the ion transport through the membrane depending on the electrolyte and glucose concentrations. At low electrolyte concentration, experimental transition times are found to be smaller in presence of glucose, which has been related to an effective membrane area reduction in presence of glucose. The membrane system corresponding to the mixture solution shows a behavior similar to the single high concentration NaCl membrane system, indicating that the observed behavior is mainly associated to the Na^+ ions transport in higher proportion. In this case, the glucose presence does not affect significantly the investigated properties of the membrane, which is interesting for its utilization in a glucose fuel cell.

Keywords: Chronopotentiometry; Transport properties; Limiting current density; Glucose; Nafion;

1. Introduction

Glucose measurement has attracted considerable interest due to its potential application in several areas such as the development of glucose sensors, waste water treatment, food industries and environmental monitoring [1-4]. On the other hand, the importance of electrochemical oxidation of sugars has been emphasized in the fields of analytical chemistry, and microbial electrochemical [5] and fuel cell technologies [6,7]. Glucose is one major biomass component that potentially possesses a large density of chemical energy. It is the fuel of many living organisms and plants. The conversion of chemical energy into electrical energy by glucose fuel cell is seriously considered. It can provide up to 16 kWs per gram generating 12 electrons per molecule during the oxidation processes [7]. A glucose fuel cell is a subtype of conventional fuel cells (using hydrogen or alcohols as fuels) that oxidizes glucose and reduces oxygen to give electric energy. Taking into account that glucose and oxygen are both present in physiological fluid, glucose fuel cell can power implanted medical devices [8]. Many battery-powered implantable medical devices have been developed for treatment ranging from neurological disorders to hearing loss. Concerning the power supply of such devices, numerous efforts have been made to develop small power-supply devices, able to operate independently over prolonged periods of time without the need of surgical replacements. Glucose fuel cells present an alternative since glucose and oxygen are both present and continuously replenished in physiological fluids by the metabolism. Beside the development of novel membranes [9], other approaches have been also investigated, as alkaline direct glucose fuel cell using anion-exchange membranes [10,11], abiotic glucose/air alkaline fuel cells [12,13], bioimplantable fuel cells based on enzymatic catalysis [14], microbial fuel cells [15] or membraneless glucose fuel cells [16]. However, despite of the numerous efforts, up to the present time, only very low electrical power production has been reported [7]. In this

challenge, proton exchange membrane is one of the essential and critical materials in fuel cells. The properties of ion-exchange membranes determine to a great extend the process performance and for this reason the choice of membranes is in fact of crucial importance. Although other alternatives are being investigated, up to new, the mostly used membrane at industrial scale is Nafion. Also microbial electrochemical technologies have not been commercialized due to various constrains including one associated with the membrane separator [5]. Nafion is biocompatible and impermeable to negatively charged proteins and presents excellent properties [8]. However, the study of the influence of neutral molecule in its transport properties has been very limited and the effect of the film morphology is still little known.

Knowledge on the morphology and internal structure of ion- exchange membranes is crucial in order to understand the manner in which the ionic transfer occurs through different conducting membranes. Studies reveal that homogeneous membrane may present micro-heterogeneities which affect their transport properties. It has been proved in the literature that electrochemical techniques like chronopotentiometry, applied to a membrane system, encompass many aspects related specifically to the membrane surface heterogeneity [17-25]. It is also important to respect some specific conditions of the electrochemical process, such as the limiting current density [26, 27].

In this paper chronopotentiometry is used to study ion transport across a Nafion membrane in presence of glucose. The aim of the work is to characterize the behavior of a Nafion membrane in media with a similar composition to human physiological fluids.

2. Experimental

2.1. Materials

2.1.1. Membrane

A commercial membrane Nafion 117 manufactured by Dupont, with a nominal equivalent weight of 1100 g/eq was used in this work. Nafion 117 is a homogeneous cation-exchange membrane consisted of a polytetrafluoreothylene backbone and a regularly spaced perfluorovinylether side chains terminated by a sulfonate ionic group. There are no cross-links in its structure. Table 1 shows some of the properties of the Nafion 117 membrane.

Table 1
Some properties of Nafion 117 membrane

Type	Homogeneous Strongly Acid Cation
Ionogenic groups	$-HSO_3^-$
Thickness, d_m (10^{-6} m)*	183
Ion-Exchange Capacity (IEC) (meq/g dry membrane)	0.94
Water Content, S (%)	23
Density, ρ_m (kgm^{-3})*	1980

*Dry membrane

2.1.2. Solutions

The materials used in the experiments were aqueous solutions of sodium and potassium chloride as electrolytes and glucose as non electrolyte. In the preparation of the solutions pure pro-analysis grade chemicals, NaCl and KCl (Merck) and glucose (Panreac), and distilled pure water were used.

First, five electrolyte solutions were prepared: two KCl solutions of concentrations 3 mol m^{-3} and 140 mol m^{-3}, other two NaCl solutions of 3 mol m^{-3} and 140 mol m^{-3}, and one mixture solution of KCl (3 mol m^{-3}) and NaCl (140 mol m^{-3}).

From each solution, other two solutions were prepared adding two different quantities of glucose: one with concentration of 0.6 g/l of glucose (named Glucose 1), and another with a glucose concentration of 0.96 g/l (named Glucose 2). Thus, 15 solutions were used: five without glucose, five with glucose 1 (0.6 g/l) and other five with glucose 2 (0.96 g/l).

This procedure permitted to ensure that the salt quantity was exactly the same for the three solutions with the same electrolyte concentration (water, glucose 1 and glucose 2).

We selected the glucose and electrolyte concentration of the solutions so that the mixture solution had similar concentration of ions and glucose than the cerebrospinal fluid (CSF) and the blood plasma.

Table 2
Ionic compositions and reference glucose content of the cerebrospinal fluid (CSF) and the blood plasma [8, 28], and of the solutions used in this study.

Fluid	CSF	Blood Plasma	This study
Na^+ ($mmol \cdot l^{-1}$)	138-150	135-145	3 and 140
K^+ ($mmol \cdot l^{-1}$)	2.7-3.9	3.6-4.8	3 and 140
Glucose ($mmol \cdot l^{-1}$)	1.1-4.4	3.9-5.5	3.3 and 5.3

2.2. Methods

2.2.1. Measurement of the electrical conductivity of the solutions

The electric conductivity of the solutions was measured using a conductivity meter JENCO Model 1671. Closed vessels containing each solution were immersed in a thermal bath at 36.1 ºC of temperature. Once the thermal equilibrium was reached, the conductivity of the solutions was measured using a suitable conductivity probe. The accuracy of the measure was 1 and 10 μScm^{-1} in the low and high electrolyte concentration intervals, respectively.

2.2.2. Measurement of swelling properties of the membrane

The solvent uptake of the Nafion 117 membrane in the different solutions was determined using the traditional gravimetric method. Before the experiments, the membrane samples were dried under vacuum for 24 h and weighted in a high precision balance (±0.0001g). After that, the samples were immersed in closed bottles containing the corresponding solution and allowed to equilibrate at 36.1 ºC. This temperature was

selected as average temperature of the human body. After 48 h of immersion the swollen membranes were taken out from the solutions, wiped carefully with filter paper in order to remove remained water drops, and weighted again. The increase in weight was equal to the weight of the liquid absorbed by the membrane. The solvent uptake (%) was calculated from the weight of the swollen and dry membrane samples according to the expression:

$$S(\%) = \frac{m_w - m_d}{m_d} 100 \quad (1)$$

where m_w and m_d are the masses of the swollen and dry membrane, respectively.

The water content of the membrane can also be expressed as the average number of water molecules per conducting functional group, λ, determined by [29]

$$\lambda = \frac{S}{100 \text{ IEC } M_w} \quad (2)$$

where IEC, 0.94 meq·g^{-1} for the used membrane, represents the ion-exchange capacity (*i.e.* the ionizable hydrophilic functional groups content per gram of polymer) and M_w is the molecular weight of water.

The parameter considered to estimate the dimensional change of the membranes was the area of the surface sample. To determine the membrane surface expansion, samples of surface, A_d, approximately square about 20x20 mm^2 were used. The procedure was similar to the one used for determining the solvent uptake, but in this case, the length of the two sides of the sample was measured. The surface expansion (%) was calculated from the change of the area according to the following expression:

$$E(\%) = \frac{A_w - A_d}{A_d} 100 \quad (3)$$

where A_w and A_d are the areas of the swollen and dry membrane, respectively.

The reproducibility of the measurements was checked in all cases.

2.2.3 Chronopotentiometric experiments

The experimental device used in this research for chronopotentiometric experiments was similar to the one used in a previous work [30]. The main part of the device consisted in a glass cell with two equal cylindrical chambers of about $4x10^{-4}$ cm^3 each one. The membrane was vertically positioned between both chambers by means of a teflon holder. The effective area of the membrane was 9.08×10^{-4} m^2.

Each chamber was provided with three communicating orifices to the exterior. A reversible Ag/AgCl electrode with a large active surface was introduced in one of the orifice to inject the electric current. This electrode consisted of a 14-15 turn spiral wire (1-mm diameter) prepared according to a method described in detailed elsewhere [31]. Another reversible Ag/AgCl electrode was introduced in other orifice to measure the electric potential difference values. This electrode consisted in a linear Ag wire of approximately 4-mm longitude and 0.5-mm diameter, also prepared by the usual method [31]. In the last orifice of each chamber a glass L-shaped capillary tube was inserted in such a way that the horizontal segments remains at the same height in order to avoid any pressure difference between both chambers. The electric potential difference established when a constant electric current circulated through the membrane systems was measured and recorder *vs* time by means of a computer. The electrodes were corrected of possible electrode asymmetry.

All the experiments were carried out under isothermal conditions (36.1ºC). The temperature requirements were achieved by introducing the complete unit in a large thermostatic bath. The temperature was constant within ±0.1 K. The measurements were carried out in absence of stirring (natural convection).

Previously each experiment, the membrane was immersed, for a minimum of 24 hours, in the corresponding solution in order to achieve equilibrium. Once the membrane

was positioned in the cell, both chambers were filled with the corresponding solution. When the system was stabilized at the selected temperature, the experimental procedure was the following:

1. Without applied electric current, the computer program recorded values of the electric voltage difference every 10 seconds to get the device zero error.
2. After the 10 seconds, a constant electric current in the 0.2-0.3 mA interval, for 3 mol m^{-3} solutions, and in the 10-200 mA interval, for the 140 mol m^{-3} solutions, was made to pass through the membrane system during 240 seconds and the electric voltage difference was recorder *vs* time.
3. After that time, the electric current was interrupted, taking values of the electric voltage during another 480 seconds.
4. At the end, under the same experimental conditions, for each electric current value, the polarity was changed and the whole experiment was repeated to preserve the good state of the electrodes.

3. Results and Discussion

3.1. Determination of the solution diffusion coefficient

Table 3 shows the values of the electric conductivity, σ, measured for the different studied solutions. Two amount of glucose were used to simulate the composition of both cerebrospinal fluid and blood plasma. From these values, it is possible to determine the diffusion coefficient, *D*, for each solution according to the following expression [32]:

$$D = \frac{\Lambda RT}{2F^2} \tag{4}$$

where Λ is the specific conductance, defined by the expression:

$$\Lambda\left(\mathrm{Scm^2mol^{-1}}\right) = 1000\frac{\sigma\left(\mathrm{Scm^{-1}}\right)}{c\left(\mathrm{M}\right)}\,, \tag{5}$$

and c is the molar concentration of the electrolyte. The obtained results are also shown in Table 3.

Table 3
Electric conductivity (σ) and diffusion coefficient (D) for different solutions at 36.1ºC. The error in the determination of the diffusion coefficient was ±0.005 and ±0.001 m^2s^{-1}, for low and high electrolyte concentrations, respectively.

Solution		σ (Scm^{-1})	D (10^{-9} m^2s^{-1})
KCl 3 mol m^{-3}	Water	$518 \cdot 10^{-6}$	2.384
	Glucose 1	$533 \cdot 10^{-6}$	2.452
	Glucose 2	$545 \cdot 10^{-6}$	2.508
KCl 140 mol m^{-3}	Water	$21.62 \cdot 10^{-3}$	2.132
	Glucose 1	$21.59 \cdot 10^{-3}$	2.129
	Glucose 2	$21.65 \cdot 10^{-3}$	2.135
NaCl 3 mol m^{-3}	Water	$451 \cdot 10^{-6}$	2.075
	Glucose 1	$492 \cdot 10^{-6}$	2.266
	Glucose 2	$489 \cdot 10^{-6}$	2.249
Na Cl 140 mol m^{-3}	Water	$17.90 \cdot 10^{-3}$	1.765
	Glucose 1	$17.91 \cdot 10^{-3}$	1.766
	Glucose 2	$17.89 \cdot 10^{-3}$	1.764
Mixture KCl 3 mol m^{-3} NaCl 140 mol m^{-3}	Water	$18.76 \cdot 10^{-3}$	1.850
	Glucose 1	$18.53 \cdot 10^{-3}$	1.828
	Glucose 2	$18.49 \cdot 10^{-3}$	1.823

In the absence of glucose, the solution conductivity increases with the electrolyte concentration and with the ionic radius of the involved cation, as it is expected [32, 33]. The estimated values for the diffusion coefficient are in agreement with those found in literature [33]. At the same electrolyte concentration, the diffusion coefficient is lower in the case of NaCl.

When the concentration of the electrolyte is low, σ and, therefore D depend on the presence of glucose. The behavior was similar for the two studied electrolytes, with higher diffusion coefficients in presence of glucose. At high electrolyte concentration, however, the influence of the presence of glucose barely affects the diffusion coefficient. For the

mixture solution, a decrease of *D* with the presence of glucose in the solution is observed, probably due to combined effect of NaCl and KCl.

When the behavior of the diffusion coefficient is analyzed in connection with the amount of glucose, it is shown that, at low electrolyte concentration, the influence is stronger in the case of KCl, with an increase of the diffusion coefficient as increases the solution glucose concentration. For NaCl solutions, the difference of the diffusion coefficients for both quantities of glucose is very low and it could be considered within the experimental error.

The increase observed in the conductivity in presence of glucose may be related to the dehydration of the ionic species due to the presence of carbohydrates. The Stokes radius in aqueous electrolyte solutions for Na^+ and K^+ ions are 0.239 and 0.125 nm, respectively [34]. The presence of glucose affects the water structure near the sodium and potassium ions, and therefore, to their hydration sphere and the corresponding Stokes radius, implying an influence in the mobility of the ions. The Stokes radius decrease could produce a decrease in the resistance of the ion movement through the liquid, implying a higher mobility and so an increase of the conductivity [35]. This effect would be expected to be greater when the hydration of the ion is higher, which agrees with the data obtained, as the effect of the presence of glucose is higher for NaCl, where the involved cation Na^+ has a higher hydration number. The influence of the presence of glucose in the conductivity could be due to the combined effect of two factors. On one hand the ability of the carbohydrate to form stable hydrogen bond with the water, what influence to the structure thereof, affecting the hydration ions, and on the other hand the variation of the solution's viscosity when there is no electrolyte [35, 36].

3.2. Solvent uptake and surface expansion

A swelling study of the membrane, solvent uptake and surface expansion, was performed by using different solutions. Table 4 presents the obtained results. The measured error for the solvent uptake and the surface expansion was lower than 0.5 and 1 %, respectively, in the most unfavorable cases. Table 4 also shows the average number of water molecules per conducting functional group estimated from the value of *S* according to Eq. (2).

It was observed that the expansion was slightly higher in one of the dimension of the sample, so that some anisotropy of dimensional change was observed, in agreement with results found in the literature [37-39], probably due to the orientation of polymer chains toward the drawing direction [38]. Any significant influence of the solution nature in the presented anisotropy was observed.

Table 4
Solvent uptake (*S*), average number of water molecules per conducting functional group (λ), and surface expansion (*E*), of Nafion 117 membrane in different solutions.

Solution		*S* (%)	λ	*E* (%)
Without electrolyte	Water	21.9	13	21
	Glucose 1	24.7	15	27
	Glucose 2	25.4	15	22
KCl 3 mol m^{-3}	Water	13.8	8	10
	Glucose 1	13.5	8	10
	Glucose 2	17.8	10	21
KCl 140 mol m^{-3}	Water	8.2	5	5
	Glucose 1	7.3	4	5
	Glucose 2	5.5	3	5
NaCl 3 mol m^{-3}	Water	19.1	11	20
	Glucose 1	15.2	9	15
	Glucose 2	20.0	12	10
NaCl 140 mol m^{-3}	Water	15.1	9	16
	Glucose 1	14.1	8	16
	Glucose 2	13.3	8	16
Mixture KCl 3 mol m^{-3} NaCl 140 mol m^{-3}	Water	15.0	9	10
	Glucose 1	15.2	9	15
	Glucose 2	15.3	9	16

Two distinct factors are determining the water content of the membrane. They are the chemical structure of the membrane itself and the nature and concentration of the electrolyte solution in contact with the membrane. The influence of the electrolyte concentration on the swelling of an ionic membrane may be complex.

In the absence of glucose in the solution, the results obtained for solvent uptake are in agreement with previous results [37,40,41]. At a given electrolyte concentration, solvent uptake decreases when the ionic radius of the cation increases. Thus, for example, for an electrolyte concentration of 3 mol m^{-3} in absence of glucose, solvent uptake was 19.1 for NaCl, with a value of the ionic radius of 9.8 nm for the Na^+ ion, and 13.8 for KCl, where the K^+ ion has a higher ionic radius of 13.3 nm [34]. These results may be explained, based on the hydration properties of ions in the solutions, by means of a decrease of the Stokes radius when the ionic radius increases [34,42]. Therefore, the solvent uptake in the membrane depends on the hydration of ions, the more hydrated is the ion, the more are the solvent uptake and the surface expansion. For the more hydrated Na^+ ion, membrane presented higher values of the solvent uptake. For a given electrolyte, solvent uptake decreases as increases electrolyte concentration. Thus, for example, in the case of NaCl with glucose 1, solvent uptakes was 15.2 with 3 mol m^{-3}, higher than with 140 mol m^{-3}, with a solvent uptake of 14.1 The reason is that as increasing concentration of external solution the osmotic pressure increases, while that in the internal solution of the membrane grows only to a small extent, since the ionic force changes a little [43].

In the absence of electrolyte, the membrane solvent uptake increases with the presence of glucose. Because of the membrane swelling properties depends on the balance between inner osmotic pressure and the associated forces with the elasticity of the polymeric matrix, the results could be due to the presence of glucose increases the

difference between the pressure in the membrane phase and solution and so favors the solvent uptake.

The influence of the type of electrolyte is similar to the one described in the case of solutions without glucose, and the swelling increases with the Stokes radius of the cation. The influence of the electrolyte concentration is also similar and the solvent uptake is lower for the solution with higher concentration of electrolyte.

However, the influence of the glucose proportion on the membrane uptake depends on both type and concentration of the electrolyte. In the case of KCl, solvent uptake increases as increases the glucose content when the concentration of the electrolyte is low, but the opposite trend is observed with the high concentration solution. A similar behavior was observed at high concentration of the NaCl, but for the lower concentration of this electrolyte a minimum is observed with Glucose 1. There is nearly no influence of the presence of glucose in the mixture solution. Although the behavior is similar for the surface expansion of the membrane, the influence is less significant and, although in general at higher water uptake, higher expansion are observed in absence of glucose, a clear relation between solvent uptake and expansion is not observed in all cases. It could indicate that changes in the thickness of the membrane happen when it is immersed in the solution. The expansion of the membrane is higher in absence of electrolyte. In presence of electrolyte, the membrane expansion is higher in NaCl solutions. At high electrolyte concentration, the membrane expansion is not influenced by the presence of glucose. At low electrolyte concentration, differences are observed between NaCl and KCl. In NaCl solutions, the presence of glucose decreases the deformation while an increase is observed in KCl solutions. It seems to indicate that the presence of glucose affects the elastic properties of the membrane. Ribeiro *et al*. [35] observed that interactions occurred between copper (II) and glucose. It is possible that interactions between counter-ions and glucose

molecules occurs, affecting the interaction between counter-ions and the fixes group of the membrane.

The membrane void porosity φ (volume of free solution within the membrane per unit volume of wet membrane) can be expressed as a function of the solvent uptake S as follows [44, 45]:

$$\varphi = \left[1 + \frac{100\rho_l}{S\rho_m} \right]^{-1} \tag{6}$$

where ρ_m and ρ_l are the densities of the dry membrane and the sorbed liquid, respectively.

At the working temperature, for the electrolyte and glucose concentrations used in this work, we can consider the value of the density of pure water at the working temperature (0.99 gcm^{-3}) for the density of all the used solutions [46] to estimate the membrane porosity from Eq. (6). The results are presented in Table 5.

The ion-exchange capacity, indicating the density of ionizable hydrophilic functional groups in the membrane, strongly affects the ion transfer. However, it is not taken into account the swelling properties of the polymer. A more appropriate measure of the true concentration of fixed charge groups is the concentration of the fixed ions groups of the membrane per volume of swollen membrane, $\overline{X}$. This parameter depends on both, membrane and solution, and can be estimated from the ion-exchange capacity, solvent uptake and porosity of the membrane, and the density of the absorbed liquid, from the equation [44]:

$$\overline{X} = \frac{100\varphi \mathrm{IEC}\rho_l}{S} \tag{7}$$

The $\overline{X}$ values estimated for all membranes systems are also shown in Table 5.

Table 5

Porosity (φ) and volumetric fixed charge concentration ($\overline{X}$), obtained for Nafion 117 membrane with different solutions.

Solution		φ	$\overline{X}$ (mol m^{-3})
Without electrolyte	Water	0.30	1.29
	Glucose 1	0.33	1.24
	Glucose 2	0.34	1.23
KCl 3 mol m^{-3}	Water	0.22	1.46
	Glucose 1	0.21	1.46
	Glucose 2	0.26	1.37
KCl 140 mol m^{-3}	Water	0.14	1.60
	Glucose 1	0.13	1.62
	Glucose 2	0.10	1.68
NaCl 3 mol m^{-3}	Water	0.28	1.35
	Glucose 1	0.23	1.43
	Glucose 2	0.29	1.33
Na Cl 140 mol m^{-3}	Water	0.23	1.43
	Glucose 1	0.22	1.45
	Glucose 2	0.21	1.47
Mixture KCl 3 mol m^{-3} NaCl 140 mol m^{-3}	Water	0.23	1.43
	Glucose 1	0.23	1.43
	Glucose 2	0.23	1.43

As can be observed, the presence of the glucose in the solution affects the membrane porosity, and the influence depends on the type and concentration of the electrolyte. In the absence of electrolyte, the membrane porosity increases in presence of glucose, and the higher concentration of glucose in the solution, the higher membrane porosity. The trend is the opposite at high electrolyte concentration, and the membrane presents a lower porosity in presence of glucose with a decrease with the glucose content. At low electrolyte concentrations, a clearly defined trend is not observed. The membrane porosity is slightly lower for low glucose concentration, but higher for high glucose concentration. For the mixture solution, the presence of glucose does not affect the membrane porosity. As a consequence, the molar fixed charge concentration increases as increases glucose concentration at high electrolyte concentration, and has not a clearly

trend at low electrolyte concentration. For the mixture solution, no change of $\overline{X}$ is observed in presence of glucose. Thus, for the mixture solution, it is expected that membrane transport properties depending on the membrane fixed charge would not be affected by changes in this parameter due to the presence of glucose.

3.3. Electrochemical characterization of the membranes

3.3.1. Curves V-t

The chronopotentiometric curves obtained for the investigated membrane systems are shown in Fig.1.

The electric current was applied in the interval 0.2-0.3 mA for 3 mol m^{-3} solutions, and in the interval 10-200 mA for 140 mol m^{-3} and mixture solutions.

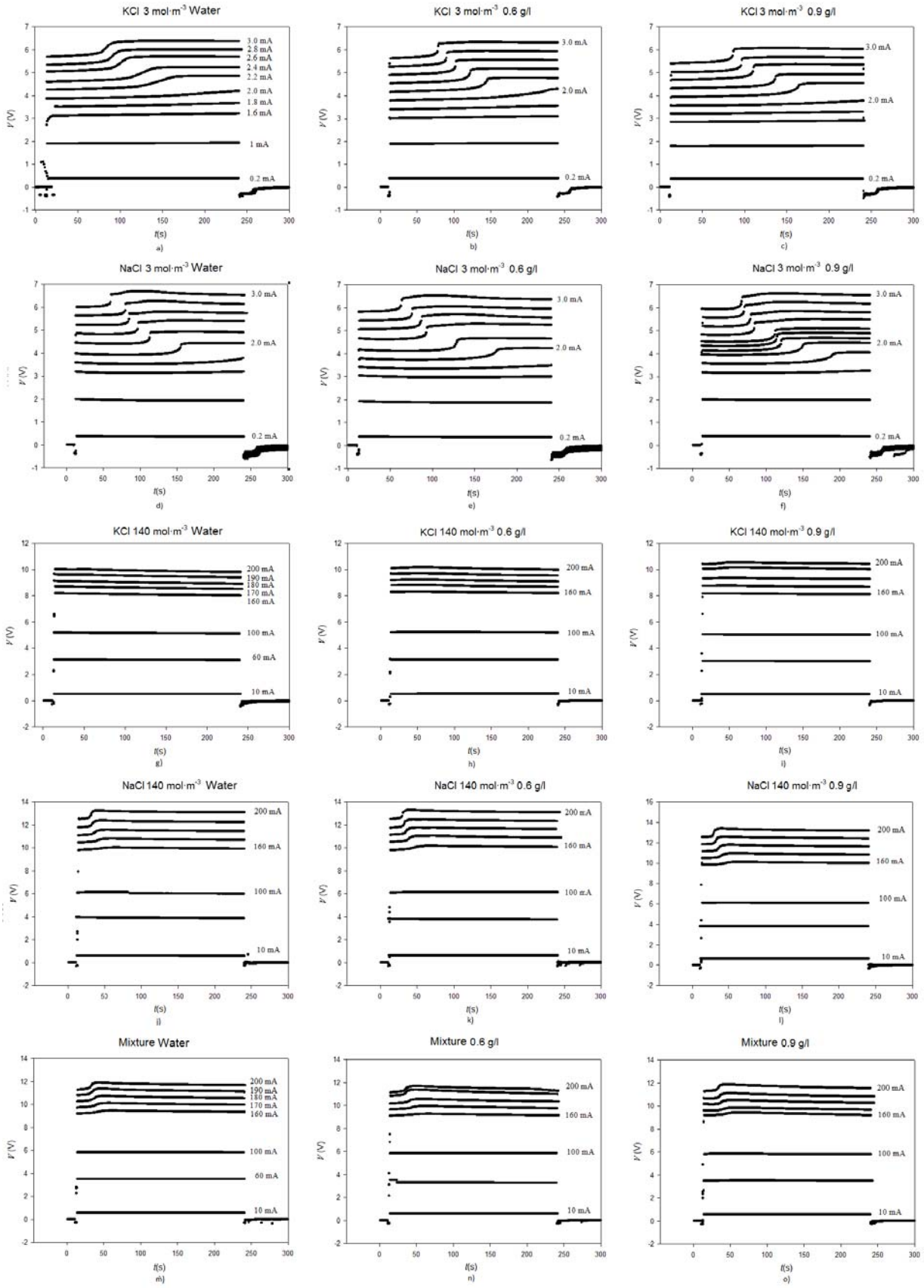

Fig. 1. Voltage-time curves at different applied electric currents for all the membrane system investigated.

The curves shown in Fig.1 exhibit the expected typical shape [24,25,47,48]. For low electric currents, when the fixed current is applied, there is an instantaneous electric voltage difference increase, V_0, which corresponds to the ohmic voltage of the membrane-solution system. In the case of 3 mol m^{-3} NaCl without glucose (Fig. 1 d), for example, the voltage increased to up 0.5 V, approximately when a current of 0.2 mA was applied. After, the voltage drop is almost constant with time until the current is switched off and a very quick drop is observed. However, when applying a current density above a certain value, the initial voltage increases in time during the application of the current. If the current density reaches a characteristic value known as limiting current density, i_L, a strong increase in voltage drop is registered. This can be observed in Fig. 1(d) for an applied electric current of 2.0 mA. This behavior is due to the permselectivity of membrane for counter-ions causes the concentration of counter-ions at the depleting electrolyte/membrane interface approaches zero. Accordingly, the limiting current density defines the transition between the range of currents corresponding to quasi-ohmic behavior and the range of currents where concentration polarization is intense and the supply of ions to the membrane surface is limited by diffusion. The time corresponding to the inflection point is named transition time τ. In the considered example of Fig. 1(d), the transition time would be around 150 s for an applied current of 2.0 mA. The decrease of the concentration in the depleting solution near the membrane is governed mainly by electrodiffusion processes. After passing the inflection point, other mechanisms of matter transfer to the membrane surface (mainly convection) become important thus leading to current densities higher than the corresponding limiting value. Note that the inflection point exists only when the current is higher than the corresponding limiting current value. If the electric current is sufficiently small, there is no drastic passage from the electrodiffusion to another transfer mechanism. Finally, the potential growth rate diminishes and the membrane

potential drop reaches a certain steady-state value or a quasi-steady-state value, V_{st}. For the considered example, the voltage increased over an initial value of 4V up to approximately 4.5 V. When the current density is switched off the voltage decreases rapidly to low values due to the relaxation of the concentration profiles in the solution boundary layer [49,50]. This trend was independent of the content of glucose in the solution.

The transition time moves to shorter times when the value of the current increases, as a consequence of the faster ion depletion in the membrane/solution interface [17,47], and depends on the membrane-solution system. It is worth mentioning the different behavior for the membrane systems with KCl 140 mol·m^3 (as shown in Fig.1 (g), (h), (i)), where the inflection point was not observed with neither applied current. It would indicate that for this membrane system, the concentration near the membrane surface does not reach zero in the study electric current interval. Fig. 1 qualitatively shows that the presence of glucose affects the electrochemical behavior of the membrane systems, depending on the nature and concentration of electrolyte. A quantitative analysis will be conducted in the next sections.

3.3.2. Determination of the limiting current for the membrane system

From the steady-state membrane potential drop, V_{st}, corresponding to each applied current in the *V-t* curves shown in Fig. 1, the current-voltage curves can be reconstituted and the limiting current density can be determined for each investigated membrane system. Fig. 2 shows, as an example, the results obtained for some of the investigated membrane systems.

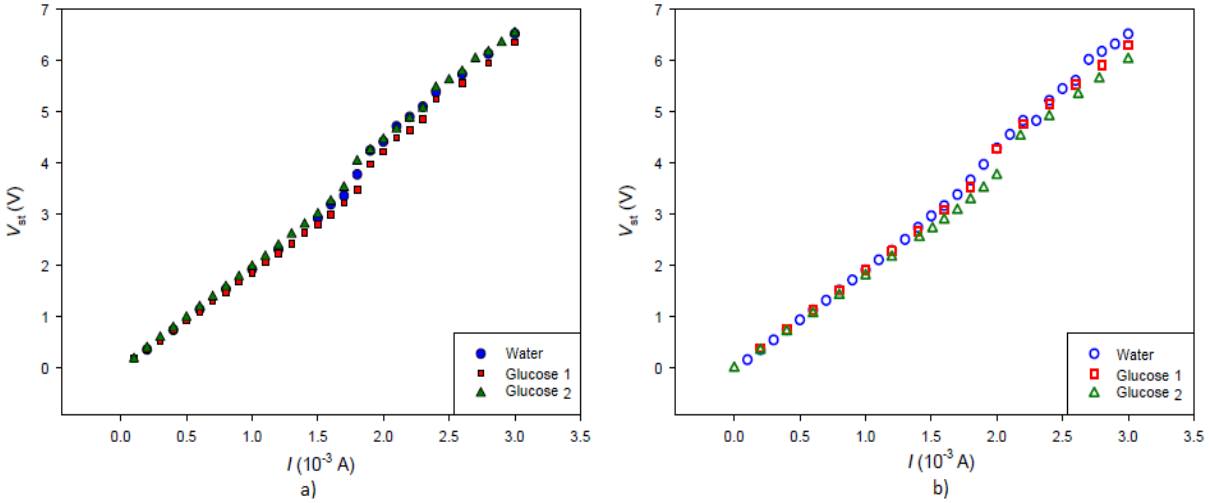

Fig. 2. V_{st}-I curves for some of the investigated membrane systems: NaCl (a) and KCl (b) solutions of 3 mol m^{-3} electrolyte concentration.

Except for the membrane system with KCl 140 mol·m^3, current-voltage curves show typical "*S*" shape with the three usual characteristic regions in this kind of membranes; a first region of approximately ohmic behavior (in Fig. 2a this region would be in the approximated interval 0-1.5 mA) a second region in which the electric current varied very slightly with the voltage (around 1.6-1.9 mA, in Fig. 2a), followed by the third region of rapid current increase (current higher than 2 mA). The second region is known as *"plateau"* and permits, by using the Cowan method [51] to obtain the value of the limiting current density, i_L, under each experimental condition. Cowan diagram is a reliable method to determine the value of the current limit when the *plateau* of the corresponding *V-I* curve is few defined, as in the studied cases [51]. According to this method, plotting *V/I vs*. I^{-1} produces a curve with two sections whose interception permits to determine the limiting current value. As an example, Fig. 3 shows the Cowan diagrams for the KCl 3 mol·m^{-3} solutions. In this case, the values obtained for the interception points were 0.63, 0.55 and 0.49 mA^{-1}, and thus the corresponding limiting currents were 1.60, 1.82 and 2.09 mA, for water, glucose 1 and glucose 2, respectively.

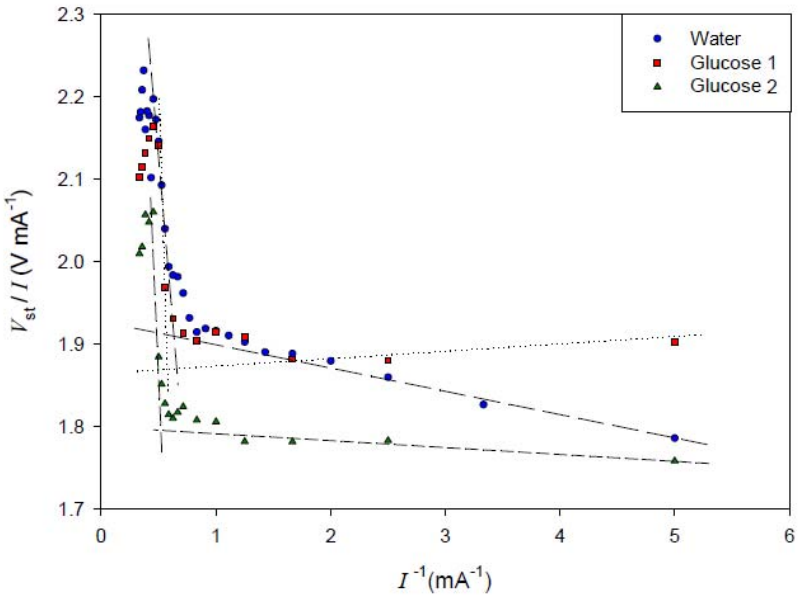

Fig. 3. Cowan diagrams. Experimental data correspond to the KCl 3 mol m^{-3} membrane system.

The systems with KCl 140 molm^3 did not present *plateau*, and a linear behavior between current and voltage was observed, indicating that the concentration polarization effect could be neglected in this case.

Table 6 shows the corresponding values of the limiting current densities obtained for each investigated membrane system, with the exception of the KCl 140 molm^3 electrolyte, for which, as it was previously said, no limiting value in the considered interval was observed. As can be observed, the obtained results are in agreement with other found in the literature for Nafion systems [25].

Table 6
Limiting current density (i_L), difference between the cationic transport numbers in the membrane and free solution (Δt_+), resistance of the membrane system before the polarization layer formation (R_0), and polarization layers thickness (δ) estimated from Eq. (9) for the studied membrane systems.

Solution		i_L (Am^{-2})	Δt_+	R_o (Ω)	δ (10^{-6} m)
KCl ….. 3 mol m^{-3}	Water	1.76	0.44	1852	890
	Glucose 1	2.00	0.36	1874	984
	Glucose 2	2.30	0.31	1781	1020
NaCl …3 mol m^{-3}	Water	1.80	0.44	1876	781
	Glucose 1	2.03	0.42	1812	724
	Glucose 2	1.89	0.36	1956	906
NaCl 140 mol m^{-3}	Water	160	0.49	60.41	305
	Glucose 1	160	0.47	60.79	318
	Glucose 2	162	0.48	60.53	307
Mixture KCl 3 mol m^{-3} NaCl 140 mol m^{-3}	Water	157	0.50	57.31	325
	Glucose 1	157	0.45	57.24	356
	Glucose 2	165	0.49	56.38	311

From the data obtained for V_{st} as a function of the applied current and the limiting current values, the ohmic resistance of the membrane system in the absence of concentration polarization effects, R_0, and the difference between the cation transport number in the membrane and in the solution, $\Delta \bar{t}_+$, can be obtained for each experimental condition examined in this study by fitting the data (V_{st}, I) by means of a minimization χ^2 method to the equation [52]:

$$V_{st} = \left(R_0 - \frac{RT}{\Delta \bar{t}_+ F I_L} \right) I + \frac{RT}{F} \left[(2\Delta \bar{t}_+) + (2\Delta \bar{t}_+)^{-1} \right] \ln \left(\frac{1+(I/I_L)}{1-(I/I_L)} \right) \quad (8)$$

where the limiting current I_L and the temperature T were considered as constant parameters, R is the universal gas constant, F the Faraday constant, and I the applied electric current. R_0, and $\Delta \bar{t}_+$ were the adjustment parameters. The obtained results are summarized in Table 6. The error in the determination of Δt_+ was about 10% and less than 2% in the determination of R_0.

Results presented in Table 6 show that the presence of glucose influences on the ionic transport through the membrane system. At a given electrolyte, the value of the limiting current density increases with the presence of glucose. However, the influence is lower for membrane systems with high electrolyte concentration. At high electrolyte concentration, the influence is only observed at the higher glucose concentration. The limiting current density is related to the difference between the counter-ion in the membrane phase and the free solution. Therefore, this result would indicate that the presence of glucose decreases the difference between the transport numbers of the transport current ions in both phases, Δt_+, and therefore, the migration of counter-ion, Na^+ and/or K^+ across membrane would be progressively reduced due to the presence of glucose with increasing concentration. It would negatively affect the permselectivity of the membrane.

The obtained results about $\Delta \bar{t}_+$ also indicate that, at low electrolyte concentration, the difference between the counter-ion mobility in the membrane and the free solution decreases with glucose, according to the results obtained for the limiting current density. Therefore, the presence of glucose would not affect equally to the ion mobility inside and outside the membrane. For 140 mol·m^{-3} NaCl, the observed differences would be already inside the experimental error, concluding that there is no dependence of the presence of glucose in the electrolyte. The ohmic resistance of the membrane system in the absence of concentration polarization effect does not present a clearly defined trend. In absence of glucose, it is higher at low electrolyte concentration. For 3 mol m^{-3} concentration is of the order of kΩ while for 140 mol m^{-3} concentration and for the mixture solution, it is of the order of 60 Ω. For a 3 mol m^{-3} electrolyte concentration, the ohmic resistance of the membrane system is higher for NaCl, with a cation of lower ionic radius. The presence of glucose only affects significantly the membrane system ohmic resistance in the case of low

electrolyte concentration. In this case, the influence of the electrolyte concentration is the same than in absence of glucose. However, the type of cation influences in a different way depending on the solution glucose amount.

According to the classical concentration polarization theory, from the values of i_L and Δt_+ shown in Table 6, and of the diffusion coefficients shown in Table 3, the thickness of the polarization layers, δ, can be estimated for each membrane system using the following equation [53]:

$$i_L = \frac{FDc_o}{\overline{\Delta t_+}\,\delta} \tag{9}$$

where c_0 is the electrolyte concentration of the solution.

Table 6 summarizes the results obtained for the layers thickness. In the absence of glucose, they are in the range expected for this kind of systems [17,21,22,26]. For a same electrolyte, the boundary layer thickness is higher at low electrolyte concentration, where polarization effects are more pronounced. The presence of glucose in the solution does not disturb this behavior and just has significant influence for the low concentrations electrolyte, where the thickness tends to increase with a higher glucose concentration in the solution. Thus, for a glucose 1 NaCl solution, the estimated polarization layer thickness was 724 μm for a 3 mol m^{-3} electrolyte concentration, while the estimated value was 318 μm for the 140 mol m^{-3} electrolyte concentration. For the NaCl 3 mol m^{-3} solution, the thickness increased to 906 μm in the case of glucose 2. The diffusion boundary layer thickness is affected by the hydrodynamics conditions of the electrolyte solution, such as the stirring rate or flow rate of the solutions. In this work the experiments have been carried out under the same hydrodynamics conditions (natural convection), so it would be expected that the boundary layer thickness would have the same value. However, data in

Table 6 show that the presence of glucose affects the hydrodynamics conditions of the system. It might be due to a decreased effective surface area of ion-exchange membrane [54]. To the purpose of check this idea, the effective fraction conducting region of the membrane has been estimated in each membrane system.

3.3.3. Determination of the effective fraction of conducting region

From the *V-t* curves, the transition time can be obtained as a function of the applied current for each membrane system. The transition time is estimated from the chronopotentiometric curve derivative, as suggested in several published works [21,55,56]. This time corresponds to the maximum point of the derivative curve and it has been determined calculating the time corresponding to the maximum value of the slope of the curve. In Fig. 4 the obtained transition times τ are shown *versus* the inverse square of the electric current density for all the membrane systems investigated.

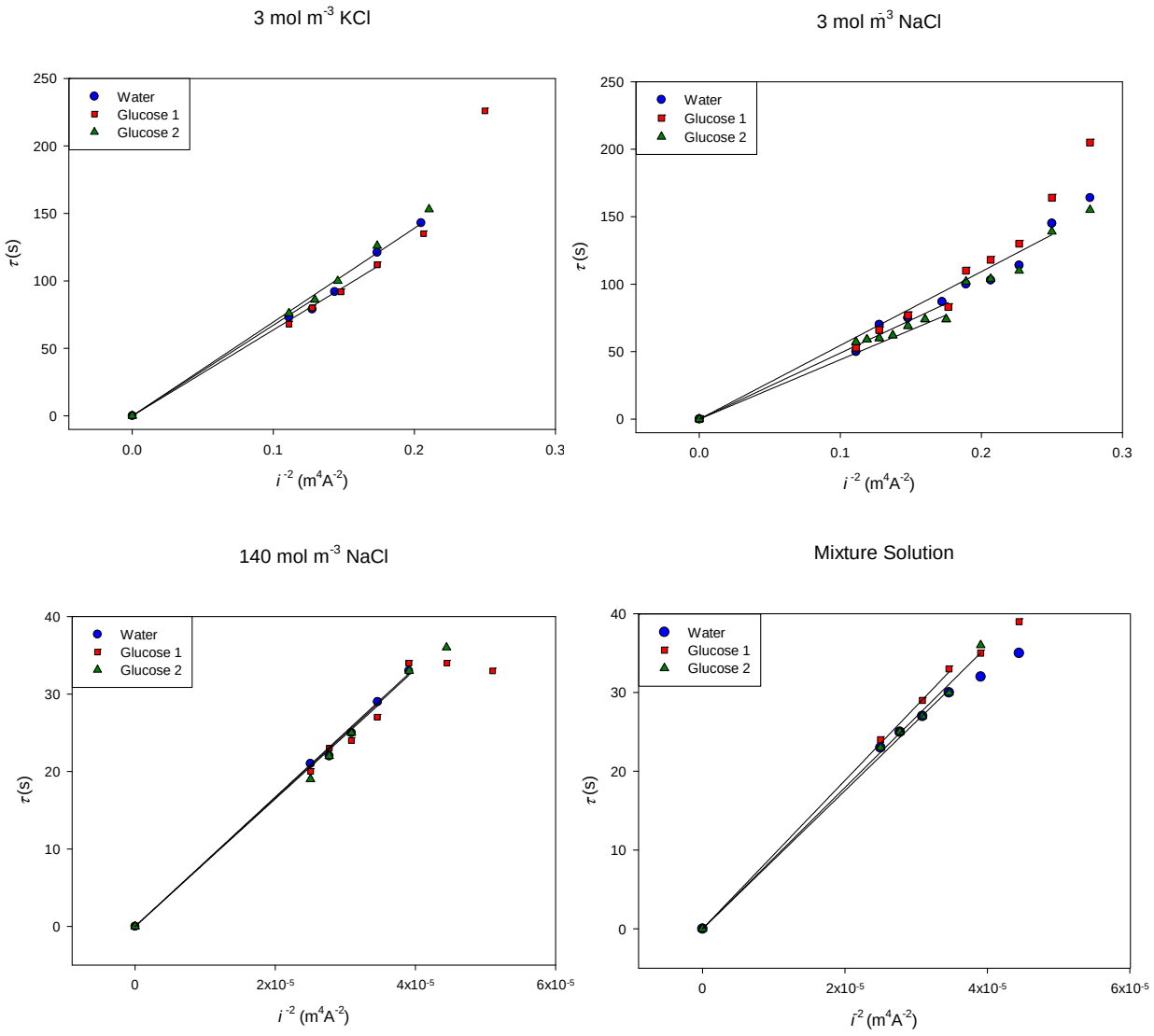

Fig. 4. Transition times for the studied membrane systems *versus* the inverse square of the electric current density.

The transition time as a function of the applied current density i is given by the Sand's equation written as follows [17]:

$$\tau = \frac{\pi D}{4}\left(\frac{c_0 F}{\bar{\Delta} t_+}\right)^2 \frac{1}{i^2} = B\frac{1}{i^2} \qquad (10)$$

where D is the solution diffusion coefficient, c_0 is the electrolyte concentration, and $\bar{\Delta} t_+$ is the difference between the cation transport numbers in the membrane and in free solution.

The validity of Eq. (10) is derivate for a semi-infinite diffusion processes. This assumes the absence of any forced or natural convection and thus an unlimited growth of

the diffusion layer next to the membrane. In this case, linear diffusion (1D diffusion) of the electrolyte through the layer adjacent to the membrane and current lines normal to the surface are considered. In the set-up used in this work with the membrane vertically positioned, there is a convective solution flow forced through the membrane creating a laminar flow diffusion layer with finite thickness, and this assumption is valid at not too large times t in which the root-mean-square displacement $(2Dt)^{1/2}$ is small compared to the thickness of the boundary layer [17,57,58]. Thus, the application of Eq. (10) would be valid for times lower than

$$t^* = \frac{\delta^2}{2D} \tag{11}$$

According to Eq. (10), in its domain of applicability and for a given concentration and for fixed values of the diffusion coefficient of electrolyte and the transport number of counter-ion in solution, the transition time would have a linear behavior *versus* the inverse of i^2, with a slope given by the parameter B dependent on membrane and solution. However, a non linear behavior appears at small current and high transitions times. In accordance with Krol *et al.* [17] this behavior is due to the imposed current, next to the limit value, does not allow the semi infinite diffusion condition needed to deduce the Sand's equation, so the diffusion layer has a finite size. Even in these conditions a finite layer can be resembled to an infinite layer if several conditions happen involving an upper limit above the transition times, and for a system with forced convention, the concentration in the polarization layers would not change for $(2D\tau)^{1/2} < \delta$. This is in agreement with the behavior observed in Fig. 4, where a linear trend is observed bellow certain time depending on the membrane system. A visual inspection of this figure permits to observe the influence of the presence of glucose.

The fit of the curves to Eq. (10) in the linear interval allows determine the value of the slope, B, of the straight lines. According to Eq. (11) and taking into account the

polarization thickness values given in Table 6, the linear interval used for fitting would be in the domains of applicability of Eq. (10). However, it is observed that the values of τi^2 estimating from the fits are not in agreement with the experimental values. As an example, for the membrane system corresponding to KCl 3 mol m^{-3} with glucose 2, Sand's equation predicts a constant value for τi^2 of 1719 $A^2s^{-1}m^{-4}$, while the mean experimental value, given by parameter B^*, is 671 $A^2s^{-1}m^{-4}$. Sand's equation was derived on the assumption that the entire membrane area is conductive and is applied to homogeneous membranes. However, heterogeneous membranes consist of conducting and not conducting regions. The current density i in Eq. (10) is a superficial current density. If the fraction of conduction is denoted as ε, the current density in the conducting region is $i^* = i/\varepsilon$. Choi *et al*. [54] modified the Sand's equation by introducing the parameter ε (so-called fraction of conduction region) to take into account the existence of non conduction regions in the membrane surface

$$i^2\tau = \pi D\varepsilon^2\left(\frac{c_0 F}{2\Delta \bar{t}_+}\right)^2 = B\varepsilon^2 = B^* \quad . \tag{12}$$

For a homogenous membrane, ε would be equal to the unity and $B^* = B$. However, even the so-called homogeneous membranes, as Nafion, considered macroscopically homogeneous are known to present non-conducting regions at the submicroscopic scale [59,60]. Table 7 shows the values obtained for parameter B^* from the fits of the transition times to Eq. (12) in the corresponding linear interval.

From the value of B^*, the diffusion coefficient D, and Δt_+, the fraction of conducting region ε could be estimated to take into account the effect of the possible membrane heterogeneities. However, as the Sand´s equation, the deduction of Eq. (12) demands the electrodiffusion should occur in the normal direction to the membrane

surface. If the surface is electrically heterogeneous, the funnel effect occurs [61] in steady state, and a tangential diffusion appears on the non-conducting regions. This tangential diffusion contribute considerably to the electrochemical behavior and the problem can no longer be considered 1D diffusion. In this case, Eq. (12) would be only applied at times lower than

$$t' = \frac{l^2}{2D} \tag{13}$$

where l is the characteristic size of surface heterogeneities. If conditions in which Eq. (12) holds are not satisfied, it would not permit to find the true fraction of conduction region ε, but it could be used as an approximation to estimate an *effective* value. Application of the Sand´s equation to the case of heterogeneous membranes shoud take into account the size of the impermeable areas [56]. The surface of a Nafion film depends strongly on the media. In water, the size of the electrical inhomogeneities of Nafion membrane surface is small comparing to the polarization layer thickness [59,60,62]. However there is no information about the effect of the presence of glucose in these inhomogeneities, and hence about the inhomogeneities size under these conditions. Thus, in this case, we must change the parameter ε in Eq. (12) for a parameter ε* which represents an effective fraction of conduction region. It can be observed that, when there is no glucose, the membrane presents effective fractions close to unity, as expected of a homogeneous membrane. The obtained values are similar to other found in literature for similar homogeneous cation-exchange membranes [17,18,25].

Table 7
Parameter B^*, effective fraction of conducting region, ε^* , local limiting current density, I_L^{Lo}, and effective polarization layer thickness, δ^{Lo}, for each solution.

Solution		B^* ($A^2s^{-1}m^{-4}$)	ε^*	i_L^{Lo} ($A\ m^{-2}$)	δ^{Lo} (10^{-6} m)
KCl 3 mol m^{-3}	Water	695±9	0.93	1.90	824
	Glucose 1	636±8	0.71	2.80	703
	Glucose 2	671±10	0.63	3.68	637
NaCl 3 mol m^{-3}	Water	546±14	0.88	2.04	687
	Glucose 1	489±14	0.76	2.67	551
	Glucose 2	440±14	0.62	3.04	562
NaCl 140 mol m^{-3}	Water	$(8.23\pm0.11)\cdot10^5$	0.88	181	270
	Glucose 1	$(8.30\pm0.12)\cdot10^5$	0.85	188	270
	Glucose 2	$(8.35\pm0.10)\cdot10^5$	0.87	186	268
Mixed KCl 3 mol m^{-3} NaCl 140 mol m^{-3}	Water	$(8.77\pm0.12)\cdot10^5$	0.90	176	289
	Glucose 1	$(9.42\pm0.12)\cdot10^5$	0.84	188	297
	Glucose 2	$(8.97\pm0.12)\cdot10^5$	0.89	186	276

At high electrolyte concentration, the influence of glucose is negligible, and the effective fraction of conducting region in the surface of the membrane is similar to in the absence of glucose. At low electrolyte concentrations, on the contrary, it is observed a decrease of the estimated effective fraction with the increase of glucose in solution, observing typical values of heterogeneous membranes.

Eq. (12) implies that the membrane contains an inert, ion impermeable region that depends on the type of solution. The reduced ion-permeable membrane area corresponds to a locally higher current density at those points where the membrane is conductive. This causes faster depletion of salt near the membrane, *i.e.* a lower transition time is observed for the membrane system. As an example, for the membrane system corresponding to KCl 3 mol m^{-3} with glucose 2 and an applied current density of 3.3 Am^{-2}, the expected transition time for a completely homogeneous considered membrane would be, according to Eq. (10), 158 s while the experimental time was 57 s. Taking into account the estimated effective fraction of conduction region, an effective local limiting current density in the conducting region, i_L^{Lo}, and an effective polarization layer thickness, δ^{Lo}, can be

calculated for each membrane system. The effective local limiting current density will be higher than the corresponding superficial value, $I_{L,}$ shown in table 6. The results are shown in Table 7. Using this value for the root-mean–square displacement, an upper limit for the transition time can be calculated using Eq. (11). Table 8 summarizes the times estimated from Eq. (11) using both values of the boundary layer thickness (superficial and local). This table also shows the corresponding experimental times.

Table 8
Times of validity of Eq. (12) t^* and t^{*Lo} determined from Eq. (11) using the boundary layer thicknesses estimated from superficial and effective local limiting current densities, respectively, and experimental values t^{exp} obtained from Fig. 4.

Solution		$\sim t^{exp}$ (s)	t^{*Lo} (s)	t^* (s)
KCl 3 mol m^{-3}	Water	143	142	166
	Glucose 1	112	101	197
	Glucose 2	86	81	207
NaCl 3 mol m^{-3}	Water	114	114	147
	Glucose 1	77	67	116
	Glucose 2	74	70	182
NaCl 140 mol m^{-3}	Water	25	21	26
	Glucose 1	30	21	29
	Glucose 2	31	20	37
Mixture KCl 3 mol m^{-3} NaCl 140 mol m^{-3}	Water	30	23	29
	Glucose 1	33	24	35
	Glucose 2	36	21	27

As can be observed, at low electrolyte concentrations there is an acceptable agreement between experimental times and times estimated from the effective layer thickness. It seems to indicate that, at low electrolyte concentration, the presence of glucose modifies the surface properties of the membrane and the corresponding limiting current density and layer thickness would correspond to those shown in Table 7. In this case, a reduced permeable membrane area corresponds to a locally higher current density at those points where the membrane is conductive. The reduction of the ionic transport could be due to the masking of ionic sites on the membrane matrix. A similar behavior was

observed by Shahi *et al*. [63] with ion-exchange membranes in presence or glycine. Park *et al*. [64] also observed a decrease of the effective fraction of conducting phase of an ion-exchange membrane in presence of bovine serum albumin as a consequence of the fouling layer deposited on the membrane surface. However, in the case of high electrolyte concentrations, the linear time interval is higher that the estimated from the effective local density current, and the experimental times better match the t^* values. It seems to indicate that the values of the limiting current density and polarization layer thickness would be those given in Table 6, and that, at high electrolyte concentration, the effective fraction of the membrane would not be practically altered by the presence of glucose, in agreement with the values of ε^* at high electrolyte concentration shown in Table 7.

The membrane system corresponding to the mixture solution showed a behavior similar to the single 140 mol m^{-3} NaCl membrane system, indicating that the observed behavior is mainly associated to the transport of Na^+ ions, with higher proportion in solution.

4. Conclusions

The ion transport properties through a Nafion membrane were studied in presence of glucose by means of chronopotentiometry. The found results showed that the addition of glucose to a sodium and potassium chloride aqueous solution affects the limiting current density and the counter-ion transport number, depending on the electrolyte and glucose concentrations of the solution. The effect of the presence of glucose was practically negligible at high electrolyte concentration, but strong at low electrolyte concentration, where a loss of membrane permselectivity was observed. In this latter case, an increase of the boundary polarization layer thickness was observed with the increase of the glucose

content in the solution, indicating that the presence of glucose affects the hydrodynamics conditions of the membrane system.

Transition times were determined as a function of the applied current density for the different membrane systems. Experimental transition times were found to be smaller than the corresponding to an ideally permselective membrane, indicating a reduced permeable membrane area. By using the modified Sand's equation, an effective fraction of conduction region has been estimated. The obtained results showed that the presence of glucose decreases the effective fraction of conducting region at low electrolyte concentration, but it does not affect the effective membrane area at high electrolyte concentration.

A study of the swelling properties of the membrane in aqueous glucose-electrolyte solutions was carried out. Nafion membrane exhibited higher water contents in absence of electrolyte, increasing the water uptake as increases the glucose content. In electrolyte solutions, the key factors were the type and concentration of the electrolyte. Liquid uptake slightly decreased with the presence of glucose at high electrolyte concentration, and had not a clearly trend at low concentration.

No significant correlation was observed between porosity and effective conducting fraction of the membrane, although both properties were affected by the presence of glucose at low electrolyte concentrations. However, the presence of glucose did not affect any of these properties at high electrolyte concentrations.

A mixture solution with a composition in NaCl, KCl, and glucose similar to the cerebrospinal fluid and blood plasma was also studied. The results showed that the presence of glucose does not affect significantly the investigated Nafion properties, which is interesting from the point of view of its utilization as solid electrolyte in a direct fuel cell using glucose in the cerebrospinal fluid.

Acknowledgements

The authors would be like to thank the anonymous reviewers for their valuable comments and suggestions to improve the quality of the paper. Financial support of this work by Banco de Santander and Universidad Complutense de Madrid within the framework of Projects 910358 and 910305 UCM Research Group-GR3/14 is gratefully acknowledged.

References

[1] T. Alizadeh, S. Mirzagholipur, A Nafion-free non-enzymatic amperometric glucose sensor based on copper oxide nanoparticles-graphene nanocomposite, Sensor and Actuators B 198 (2014) 438-447.

[2] K. E. Toghill, R. G. Compton, Electrochemical non-enzymatic glucose sensor: a perspective and an evaluation, Int. J. Electrochem. Sci. 5 (2010) 1246-1301.

0[3] L. Meng, J. Jing, G. Yang, T. Lu, H. Zhang, C. Cai, Nonenzymatic electrochemical detection of glucose based on palladium-single-walled carbon nanotube hybrid nanostructures, Anal. Chem. 81 (2009) 7271-7280.

[4] D. Chen, C. Wang, W. Chen, Y. Chen, J. X.J. Zhang, PVDF-Nafion nanomembranes coated microneedles for *in vivo* transcutaneous implantable glucose sensing, Biosens. Bioelectron. 74 (2015) 1047-1052.

[5] S. M. Daud, B. H. Kim, M. Ghasemi, W. R. W. Daud, Separators used in microbial electrochemical technologies: Current status and future prospects, Bioresource Technol. 195 (2015) 170-179.

[6] K. Elouarzaki, R. Haddad, M. Holzinger, A. L. Goff, J. Thery, S. Cosnier, MWCNT-supported phthalocyanine cobalt as air-breathing cathodic catalyst in glucose/O_2 fuel cells, J. Power Sources 255 (2014) 24-28.

[7] S. Cosnier, A. Le Goff, M. Holzinger, Towards glucose biofuel cells implanted in human body for powering artificial organs: Review, Electrochem. Commun. 38 (2014) 19-23.

[8] B. I. Rapoport, J. T. Kedzierski, R. Sarpeshkar, A glucose fuel cell for implantable brain-machine interfaces, PloS ONE 7(6) (2012) e38436.

[9] G-P Jiang, J. Zhang, J-L. Qiao, Y-M. Jiang, H. Zarrin, Z. Chen, F. Hong, Bacterial nanocellulose/Nafion composite membranes for low temperature polymer electrolyte fuel cells, J. Power Sources 273 (2015) 697-706.

[10] Y-L. Yang, X-H. Liu, M-Q. Hao, P-P. Zhang, Performance of a low-cost direct glucose fuel cell with an anion-exchange membrane, Int. J. Hydrogen Energy 40 (2015) 10979-10984.

[11] R. Haddad, J. Thery, B. Gauthier-Manuel, K. Elouarzaki, M. Holzinger, A. Le Goff, G. Gautier, J. E. Mansouri, A. Martinent, S. Cosnier, High performance miniature glucose/O_2 fuel cell based on porous silicon anion exchange membrane, Electrochem. Commun. 54 (2015) 10-13.

[12] D. Orton, D. Scott, Temperature dependence of an abiotic glucose/air alkaline fuel cell, J. Power Sources 295 (2015) 92-98.

[13] S. Kerzennmacher, J. Ducrée, R. Zengerle, F. von Stetten, Energy harvesting by implantable abiotically catalized glucose fuel cell. J. Power Sources 182 (2009) 1-17.

[14] A. Heller, Miniature biofuel cells, Phys. Chem. Chem. Phys. 6 (2004)-209-216.

[15] B. E. Logan, Microbial Fuel Cells, Hoboken, New Jersey, John Wiley and Sons, 2008

[16] G. Slaughter, J. Sunday, A membraneless single compartment abiotic glucose fuel cell, J. Power Sources 261 (2014) 332-336.

[17] J. J. Krol, M. Wessling, H. Strathmann, Chronopotentiometry and overlimiting ion transport through monopolar ion exchange membranes, J. Membr. Sci. 162 (1999) 155-164.

[18] J-H. Choi, S-H. Moon, Pore size characterization of cation-exchange membranes by chronopontentiometry using homologous amine ions, J. Membr. Sci. 191 (2001) 225-236.

[19] R. K. Nagarale, V. K. Shahi, S. K. Thampy, R. Rangarajan, Studies on electrochemical characterization of polycarbonate and polysulfone based heterogeneous cation-exchange membranes, React. Funct. Polym. 61 (2004) 131-138.

[20] L. X. Tuan, M. Verbanck, C. Buess-Herman, H. D. Hurwitz, Properties of CMV cation exchange membranes in sulfuric acid media, J. Membr. Sci. 284 (2006) 67-78

[21] N. D. Pismenskaya, V.V. Nikonenko, E. I. Belova, G. Y. Lopatkova, P. Sistat, G. Pourcelly, K. Larshe, Coupled convection of solution near the surface of ion-exchange membranes in intensive current regimes, Russ. J. Electrochem. 43 (2007) 307-327.

[22] M. Sidorova, L. Ermakova, A. Kiprianova, D. Aleksandrov, S. Timofeev, Electrochemical characteristics and concentration polarization of perfluorinated cation-exchange membranes, Adv. Colloid Interface Sci. 134-135 (2007) 224-235.

[23] J. M. Zook, S. Bodor, R. E. Gyurcsányi, E. Lindner, Interpretation of chronopotentiometric transients of ion-selective membranes with two transition times, J. Electroanal. Chem. 638 (2010) 254-261.

[24] I. Herraiz-Cardona, E. Ortega, V. Pérez-Herranz, Evaluation of the Zn^{2+} transport properties through a cation-exchange membrane by chronopotentiometry. J. Colloid Interface Sci. 341 (2010) 380-385.

[25] M. C. Martí-Calatayud, D.C. Buzzi, M. García-Gabaldón, A.M. Bernardes, J.A.S. Tenório, V. Pérez-Herranz, Ion transport through homogeneous and heterogeneous ion-

exchange membranes in single salt and multicomponent electrolyte solutions, J. Membr. Sci. 466 (2014) 45-57.

[26] V.V. Nikonenko, N. D. Pismenskaya, E. I. Belova, P. Sistat, P. Huguet, G. Pourcelly, C. Larchet, Intensive current transfer in membrane systems: Modelling, mechanisms, and application in electrodialysis, Adv. Colloid Interface Sci. 160 (2010) 101-123.

[27] N. D. Pismenskaya, V.V. Nikonenko, N. A. Melnik, K. A. Shevtsova, E. I. Belova, G. Pourcelly, D. Cot, L. Dammak, C. Larchet, Evolution with time of hydrophobicity and microrelief of a cation-exchange membrane surface and its impact on overlimiting mass transfer, J. Phys. Chem. B 116 (2012) 2145-2161.

[28] H. Reiber, M. Ruff, M. Uhr, Ascorbate concentration in human cerebrospinal fluid (CSF) and serum. Intrathecal accumulation and CSF flow Rate, Clin. Chim. Acta 217 (1993) 155-164.

[29] Y. S. Li, T. S Zhao, W.W. Yang, Measurements of water uptake and transport properties in anion-exchange membranes, Int. J. Hydrogen Energy 35 (2010) 5656-5665.

[30] V.M. Barragán, C. Ruiz-Bauzá, J.P.G. Villaluenga, B. Seoane, On the methanol-water electroosmotic transport in a Nafion membrane, J. Membr. Sci. 236 (2004) 109-120.

[31] G. J. Janz, Silver-Silver Halide Electrodes, in: D. J. G. Ives, G. J. Janz (Eds.), Reference Electrodes, Academic Press, London, 1961, pp.179.

[32] J. O´M. Bockris, A.K.N. Reddy, Modern Electrochemistry. Vol 1. Plenum Press, New York, 1970.

[33] V. M. M. Lobo, Electrolyte solutions: Literature data on thermodynamic and transport properties, Coimbra Editora, Coimbra, 1975.

[34]P.C.F. Pau, J. O. Berg, W. G. McMillan, Application of Stokes´ law to ions in aqueous solutions, J. Phys. Chem. 94 (1990) 2671-2679.

[35] A. C. F. Ribeiro, M. A. Esteso, V. M. M. Lobo, A. J. M. Valente, S. M. N. Simões, A. J. F. N. Sobral, H. D. Burrows, Interactions of copper (II) chloride with sucrose, glucose, and fructose in aqueous solutions, J. Mol. Struct. 826 (2007) 113-119.

[36] R. Z. Sabirov, O. V. Krasilnikov, V. I. Ternovsky, P. G. Merzliak, Relation between ionic channel conductance and conductivity of media containing different electrolytes. A novel method of pore determination, Gen. Physiol. Biophys. 12 (1993) 95-111.

[37] A. Randová, S. Hovorka, P. Izák, L. Bartovská, Swelling of Nafion in methanol-water-inorganic salt ternary mixtures, J. Electroanal. Chem. 616 (2008) 117-121.

[38] D. R. Morris, X. Sun, Water-sorption and transport properties of Nafion 117, J. Appl. Polym. Sci. 50 (1993) 1445-1442.

[39] V. M. Barragán, S. Muñoz, Influence of a Microwave irradiation on the swelling and permeation properties of a Nafion membrane, J. Membrane Sep. Technol. 4 (2015) 32-39.

[40] I. A. Stenina, Ph. Sistat, A. I. Rebrov, G. Pourcelly, A. B. Yaroslavtsev, Ion mobility in Nafion-117 membranes, Desalination 170 (2004) 49-57.

[41] V. M. Barragán, M. J. Pérez-Haro, Correlations between water uptake and effective fixed charge concentration at high univalent electrolyte concentrations in sulfonated polymer cation-exchange membranes with different morphology, Electrochim. Acta 56 (2011) 8360-8367.

[42] M. Y. Kiriukhim, K. D. Kollins, Dymanic hydration numbers for biologically important ions, Biophys. Chem. 99 (2002) 155-168.

[43] F. G. Helfferich, Ion-Exchange, Dover, London, 1962.

[44] A. Lehmani, P. Turq, M. Périé, J. Périé, J-P. Simonin, Ion transport in Nafion 117 membrane, J. Electroanal. Chem. 428 (1997) 81-89.

[45] P. Somovilla, J.P. G. Villaluenga, V.M. Barragán, M.A. Izquierdo-Gil, Experimental determination of the streaming potential across cation-exchange membranes with different morphologies, J. Membr. Sci. 500 (2016) 16-24.

[46] J. F. Comesaña, J. J. Otero, E. García, A. Correa, Densities and viscosities of Ternary Systems of Water+ glucose +sodium chloride at several temperatures, J. Chem. Eng. Data 48 (2003) 362-366.

[47] R. Ibanez, D.F. Stamatialis, M. Wessling, Role of membrane surface in concentration polarization at cation exchange membranes, J. Membr. Sci. 239 (2004) 119-128.

[48] L. Marder, E. M. O. Navarro, V. Pérez-Herranz, A. M. Bernardes, J. Z. Ferreira, Chronopotentiometric study on the effect of boric acid in the nickel transport properties through a cation-exchange membrane, Desalination 249 (2009) 348-352

[49] S. Grzegorczyn, A. Slezak, Time characteristics of electromotive force in single-membrane cell for stable and unstable conditions of reconstructing of concentration boundary layers, J. Membr. Sci. 280 (2006) 485-493.

[50] C. Larchet, S. Nouri, B. Auclair, L. Dammak, V.V. Nikonenko, Application of chronopotentiometry to determine the thickness of diffusion layer adjacent to an ion-exchange membrane under natural convention, Adv. Colloid Interface Sci. 139 (2008) 45-61.

[51] C. Ponce-de-León, C. T. J. Low, G. Kear, F. C. Walsh, Strategies for the determination of the convective-diffusion limiting current from steady state linear sweep voltammetry, J. Appl. Electrochem. 37 (2007) 1261-1270.

[52] V. M. Barragán, C. Ruiz-Bauzá, Current-voltage curves for ion-exchange membranes: a method for determining the limiting current density, J. Colloid Interface Sci. 205 (1998) 365-373.

[53] H. Strathmann, Ion-Exchange Membrane Separation Processes, Membrane Science and Technology Series, 9, Elsevier, Amsterdam, 2004.

[54] J-H. Choi, S-H. Kim, S-H. Moon, Heterogeneity of ion-exchange membranes: the effect of membrane heterogeneity on transport properties, J. Colloid Interface Sci. 241 (2001) 120-126.

[55] N. Pismenskaia, P. Sistat, P. Huguet, V.V. Nikonenko, G. Pourcelly, Chronopotentiometric applied to the study of ion transfer through anion exchange membranes, J. Membr. Sci. 228 (2004) 65-76.

[56] X. L. Le, P. Viel, D.P. Tran, F. Grisotto, S. Palacin, Surface homogeneity of anion exchange membranes: a chronopotentiometric study in the overlimiting current range, J. Phys. Chem. B 113 (2009) 5829-5836.

[57] S. A. Mareev, D. Y. Butylskii, N. D. Pismenskaya V. V. Nikonenko, Chronopotentiometry of ion-exchange membranes in the overlimiting current range. Transition time for a finite-length diffusion layer: modeling and experiment, J. Membr. Sci. 500 (2016) 171-179.

[58] M. V. Soestbergen, P. M. Biesheuvel, M. Z. Bazant, Phys. Rev. E 81 (2010) 021503-1-13.

[59] W.Y. Hsu, T.D. Gierke, Ion transport and clustering in nafion perfluorinated membranes, J. Membr. Sci. 13 (1983) 307-326.

[60] K. Mauritz, R. Moore, State of understanding of Nafion, Chem. Rev. 104 (2004) 4535-4585.

[61] I. Rubinstein, B. Zaltzmann, T. Pundik, Ion-exchange funneling in thin-film coating modification of heterogeneous electrodialysis membranes, Phys. Rev. E, 65 (2002) 041507-1-9.

[62] M. Bass, A. Berman, A. Singhn, O. Konovalov, V. Freger, Macromolecules 44 (2011) 2893-2899.

[63] V. K. Shahi, S. K. Thampy, R. Rangarajan, Chronopotentiometric studies on dialytic properties of glycine across ion-exchange membranes, J. Membr. Sci. 203 (2002) 43-51.

[64] J-S. Park, J-H. Choi, K-H. Yeon, S-H. Moon, An approach to fouling characterization of an ion-exchange membrane using current-voltage relation and electrical impedance spectroscopy, J. Colloid Interface Sci. 294 (2006) 129-138.

Figure caption

Fig.1. Voltage-time curves at different applied electric currents for all the membrane system investigated.

Fig. 2. V_{st}-I curves for some of the investigated membrane systems: NaCl (a) and KCl (b) solutions of 3 mol m^{-3} electrolyte concentration.

Fig.3. Cowan diagrams. Experimental data correspond to the KCl 3 mol m^{-3} membrane system.

Fig.4. Transition times for the studied membrane systems *versus* the inverse square of the electric current density.